Technische Universität Dresden
Faculty of Environmental Sciences
Department of Hydro Science and Engineering

A Study Project Report on

Physical and Chemical Analysis of Dredging Material from the Dead Sea Environment

Submitted by:

Madhav Khatri

5125523

in March 2024

Supervisor: Prof. Dr.-Ing. Bernhard Vowinckel

Table of Contents

List of Figures

List of Tables

List of Abbreviations

APC : Arab Potash Company

BSI : British Standards Institute

DIN : Deutsches Institut für Normung

DS : Dead Sea

DSPGC : Dead Sea Preservation Government Company Ltd.

DW : Distilled Water

BW : Brine Water

EC : Electroconductivity

ICL : Israel Chemicals Ltd

ICP-MS : Inductively Coupled Plasma- Mass Spectrometer

ISSS : International Soil Science Society

MCM : Million Cubic Meters

MIT : Massachusetts Institute of Technology

rpm : Revolution per minute

USPRA : United States Public Road Association

List of Symbols

Symbol	Unit	Meaning
C_u	-	Coefficient of Uniformity
g	m/s^2	Acceleration due to gravity
V_s	m/s	Settling velocity
ρ_s	Kg/m^3	Density of halite
ρ_{DS}	Kg/m^3	Density of saturated solution
μ	Kg/(m.s)	Dynamic Viscosity of solution
r	m	Radius of salt grain
µm	-	micrometres

Abstract

The Dead Sea, renowned for its extreme salinity and unique geological features, faces challenges related to the accumulation of salt in its evaporation ponds, posing environmental and economic concerns. This study explores the feasibility of transporting accumulated halite salt grains from these ponds to the northern Dead Sea basin via the Nahal Arava river. Laboratory analysis of halite samples reveals gran sizes ranging from 100 to 4000 microns with a median size of 1800 microns and a bulk density of approximately 1250 kg/m³. While sodium comprises 98.90% of the elemental composition, trace elements such as Fe, Mg, and Al are present at 1.1%. However, the presence of non-dissolvable particulates, indicated by turbidity in diluted salt solutions, and the detection of trace elements suggest potential challenges and increased production costs due to additional purification processes. Limited information on Nahal Arava river hinders a comprehensive feasibility study, but the findings provide valuable insights for further investigation, highlighting the need for real data on flow conditions to accurately assess transportation feasibility.

1. Introduction

The Dead Sea (DS), located at 423 meters below mean sea level, is recognized as the Earth's lowest and most saline lake (Sztankeler et al., 2012). It is bordered by Israel on the western side and Jordan on the eastern side as depicted in figure 1.1. Renowned for its exceptionally high salt content, the Dead Sea is a vital source of raw materials for the minerals industry and remains a popular destination for tourists worldwide (Al Bawab et al., 2018). There are two regions on the DS area: on the north, the DS itself and on the south, the evaporation ponds.

The extraction of potassium from the DS by Israel Chemicals Ltd (ICL) and the Arab Potash Company (APC) in Jordan serves a crucial role in meeting global fertilizer demand. Operating independently, both companies pump DS brine into evaporation ponds totalling approximately 250 km^2 (140 km^2 in Israel and 110 km^2 in Jordan (Reznik & Gavrieli, 2023).

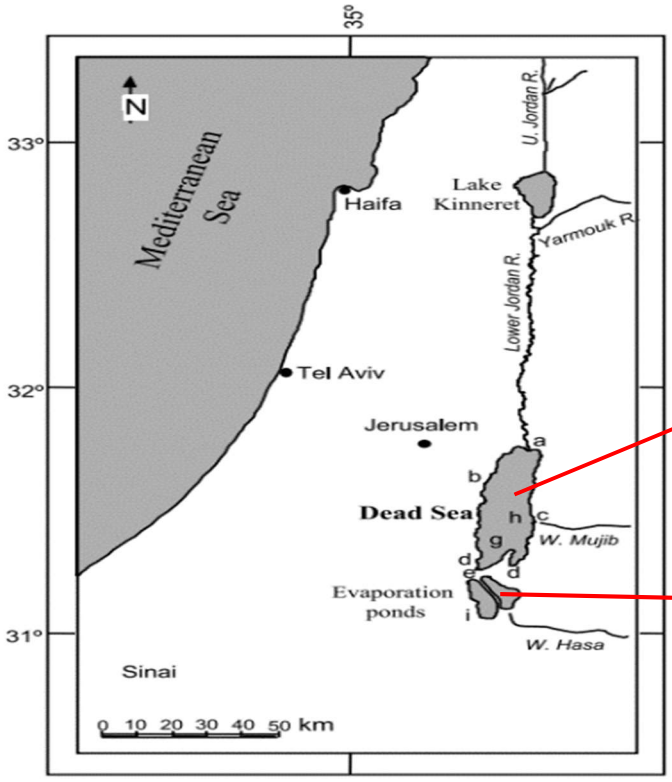

Figure 1.1: Location map of the Dead Sea (DS) region (Lensky et al., 2005)

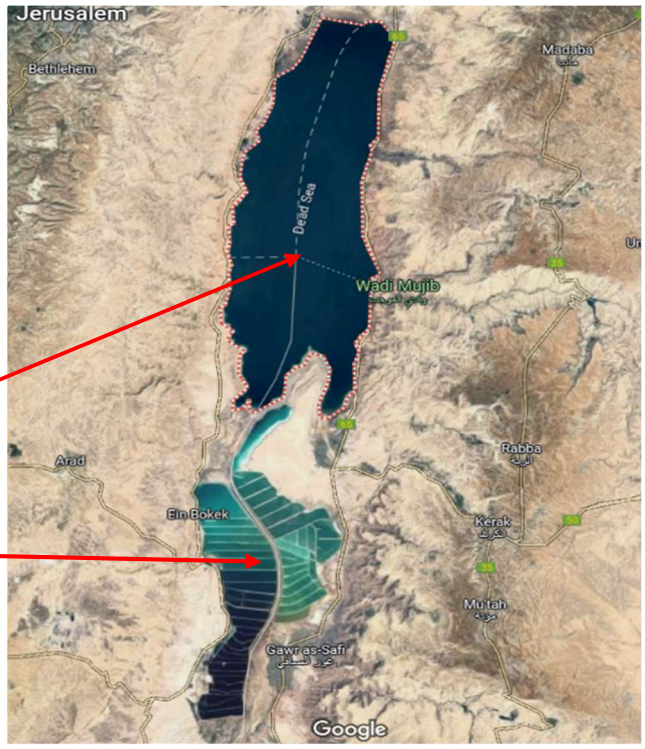

Figure 1.2: Closer view of the study area showing two regions, extracted from Google earth.

At the ICL Dead Sea site, the production process revolves around maintaining a constant volume of solutions, or brines in the evaporation ponds. Initially, the brine evaporates, precipitating halite as rock waste. Subsequently, the brine is transferred to additional ponds,

where increased salinity prompts the precipitation of carnallite, which is harvested for potash production. Annually, about 20 million tonnes of salt precipitate at the pond's bottom, creating a new 20 cm layer of salt (Gavrieli et al., 2009). These layers accumulate over time, reducing the volume of brine in the pond. However, to sustain the production process, it's imperative to maintain a fixed brine volume. Consequently, the pond's level has been steadily rising each year, aligned with the rate of floor elevation, which poses concerns for the nearby hotels situated at along the Dead Sea's shores (Abelson et al., 2009).

Recognizing the environmental implications, the Dead Sea Preservation Government Company Ltd. (DSPGC) has embarked on a study to explore solutions to this challenge. Among the prominent alternatives under consideration is the extraction of salt from the pond's bottom to stabilize its level through dredging activities. However, this approach necessitates the removal of substantial salt volumes, with harvesting the entire pond area (~80 km^2, the area of the largest evaporation pond, Pond 5) in the region) requiring an estimated 16 million cubic meters per year (MCM/y), equivalent to 400 MCM over the next 25 years (Gavrieli et al., 2009).

Figure 1.3: Closer view of the evaporation ponds showing the gradual change of colour from north to south, indicating precipitation of halite in the earlier ponds to carnallite in the subsequent ponds.

Figure 1.4: Dotted red line depicting Nahal Arava river which flows through evaporation ponds of Israel and Jordan.

The Dead Sea Enterprises, following a government directive from 2012, are pursuing a salt harvesting initiative that involves transporting salt from the evaporation ponds to the northern Dead Sea basin for burial. This project aims to address problem of accumulation of salt in the pond. However, concerns have been raised regarding the transportation of such large volumes of salt through the Lynch strait and the potential environmental impact on visibility and safety. In response, Dead Sea Enterprises are exploring alternative proposals, including using a conveyor belt across the Lynch strait to transport salt to the northern basin.

Figure 1.5: (a) Google Earth satellite view of the ICL salt piles. (b) Close-up view of the ICL salt piles. The picture faces west (Reznik & Gavrieli, 2023).

This study is done to find out if it is possible to transport the accumulated halite salt as granular material in the evaporation ponds to the DS through Nahal Arava river, which is located between the evaporation ponds of Israel and Jordan as shown by the dotted red line in figure 1.4. It runs through these evaporation ponds, all the way to DS. Physical and chemical properties of halite are studied in the laboratory to help find out the feasibility of transportation of halite salt into the northern basin.

2. Methodology

In this study, a salt sample was obtained from one of the evaporation ponds of the southern DS basin. Then further physical and chemical analyses of the salt sample were done in the chemical laboratory of Technische Universität Dresden. Following methodology was adopted.

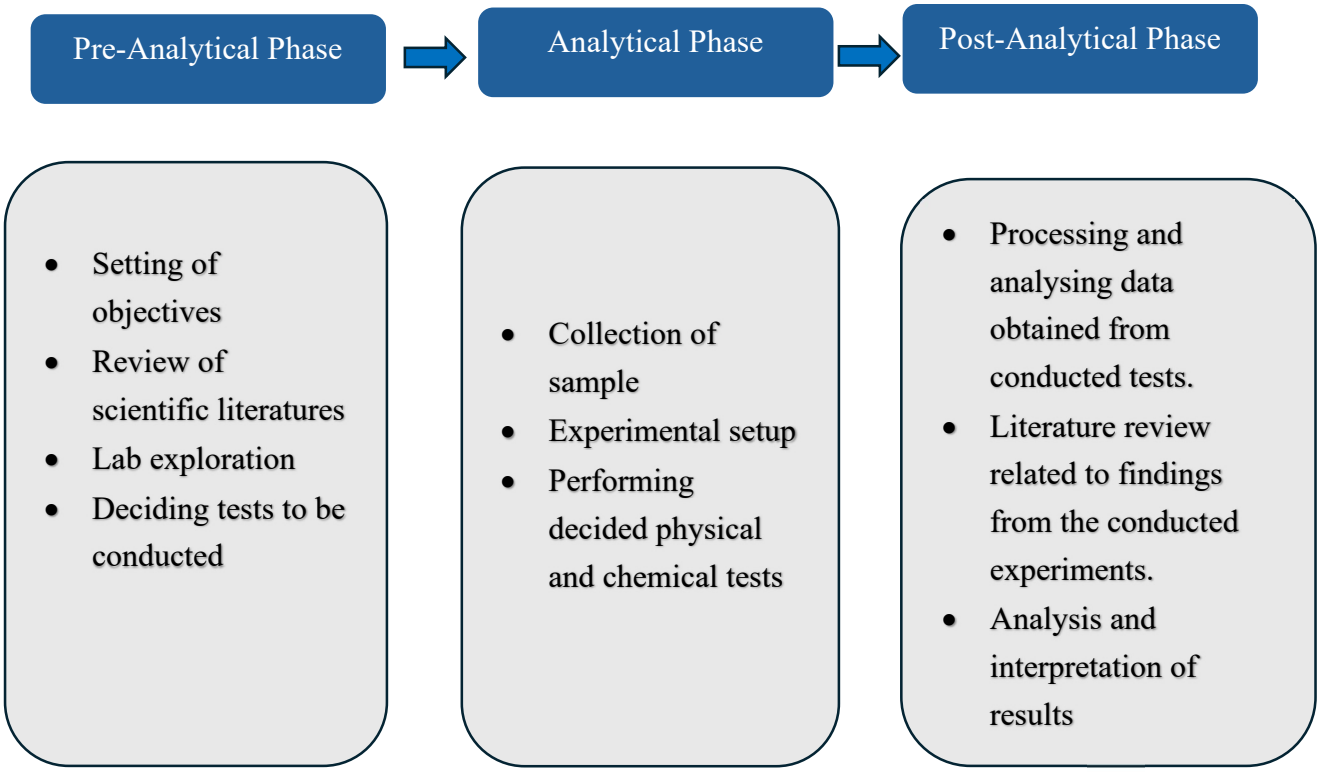

Figure 2.1: Adopted Methodology for the study project.

3. Laboratory Tests

3.1 Physical Analysis

3.1.1 Sieve analysis

Sieve analysis of the salt sample was adopted to find the grain size distribution. For this, Vibratory Sieve Shaker AS 200 CONTROL was adopted.

At first, the salt sample was set to air dry as shown in figure 3.1. To ensure the homogeneity of the sample, it was put in sample divider PT 100. A faultless and comparable analysis is closely linked to accurate sample handling. Only a sample representative of the initial material can provide meaningful analysis results. Rotating dividers ensure the representativeness of a sample and thus the reproducibility of the analysis. The sample divider PT 100 divides the sample so exactly that the composition of each fraction of the sample corresponds exactly to that of the original bulk sample. This applies both for fine-powdered and coarse materials.

After sampling, six homogenous samples were obtained. sieve sizes in the range of 100 micrometres(µm) to 4000 µm were selected. Out of the obtained six samples, three were selected and put in vibratory sieve shaker one by one, each experiment lasting for one minute. The results were plotted for the three runs.

(a) (b) (c)

Figure 3.1: (a) Air Dried Salt Sample (b) selected Sieve sizes ranging from 100 µm to 4000 µm (c)Sample divider PT 100 used for obtaining homogenous samples out of the original sample

3.1.2 Experiment on solubility of the salt sample:

For this test, salt sample was taken and added to 500 ml of distilled water (DW) gradually at an increment of 50 gram(g), while constantly stirring the salt sample at the rate of 300 revolutions per minute(rpm). Parameters like density, pH, Electroconductivity (EC) and Temperature were noted down. After stirring and continuously adding the salt, and after certain time and certain portion of added salt, the salt stopped dissolving the water and this was noted as saturation point.

3.1.3 Particle Count Analysis:

At the end of solubility experiment, the diluted salt solution was found dirty, clearly indicating traces of undissolved particles. So, a particle count analysis was done to find the fraction of undissolved particles present in the salt sample.

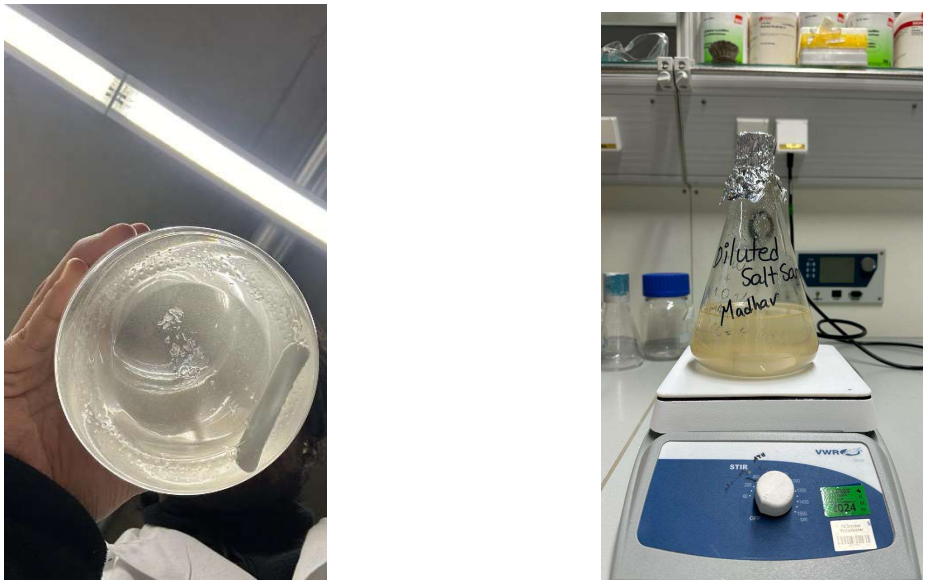

(a) (b)

Figure 3.2: (a) Figure indicating the attainment of saturation state when no more salt grains were found dissolving in the DW. The rectangular device at the bottom of flask is the magnetic stirrer. (b) Figure indicating the change in colour of the diluted salt solution, indicating the presence of undissolved particles in the salt sample.

3.2 Chemical Analysis:

3.2.1 Inductively Coupled Plasma Mass Spectrometry (ICP-MS)

ICP-MS uses an argon (Ar) plasma – the ICP – to convert the sample into ions that are then measured using a Mass Sspectrometer – the MS. An ICP-MS instrument consists of the ion source (the ICP), a mass spectrometer (MS) – usually a scanning quadrupole mass filter, and a detector. In our study, our salt sample was introduced in ICP-MS device.

ICP-MS is a sophisticated analytical technique used for the precise quantification of trace elements and isotopes in various samples. In this method, samples are introduced into a high-temperature plasma, where they are atomized and ionized. The ions generated in the plasma are then separated based on their mass-to-charge ratio using ion optics before being detected by a sensitive detector. Through the analysis of the ion signals, ICP-MS provides quantitative information on the concentration of elements and isotopes present in the sample, often at very low levels. Its high sensitivity, wide elemental coverage, and ability to handle complex sample matrices make it indispensable in fields such as environmental monitoring, geochemistry, pharmaceutical analysis, and materials science.

4. Observations, Results and Findings

4.1 Sieve Analysis

For the three runs of test conducted, following observations were made:

Table 4.1: Observation from 3 test runs

Run 1		Run 2		Run 3	
sieve size(µm	percentage passing(%)	sieve size(µm)	percentage passing(%)	sieve size(µm)	percentage passing(%)
>4000	100	>4000	100	>4000	100
4000	90.00	4000	90.76	4000	89.79
3150	78.78	3150	80.17	3150	79.26
2500	64.65	2500	65.70	2500	64.45
1800	40.96	1800	40.89	1800	39.45
1600	33.31	1600	32.83	1600	30.21
1400	26.64	1400	26.39	1400	22.94
1250	21.26	1250	20.54	1250	17.24
1000	11.81	1000	12.05	1000	6.43
800	5.06	800	6.04	800	0.99
710	2.59	710	3.32	710	0.30
630	1.37	630	1.66	630	0.11
250	0.00	250	0.00	250	0.01
100	0.00	100	0.00	100	0.00

For plotting the sieve analysis curves, sieve sizes (grain size) were plotted on logarithmic x-axis and cumulative percentage passing was plotted in the y-axis. The observations found were typical sieve analysis curves.

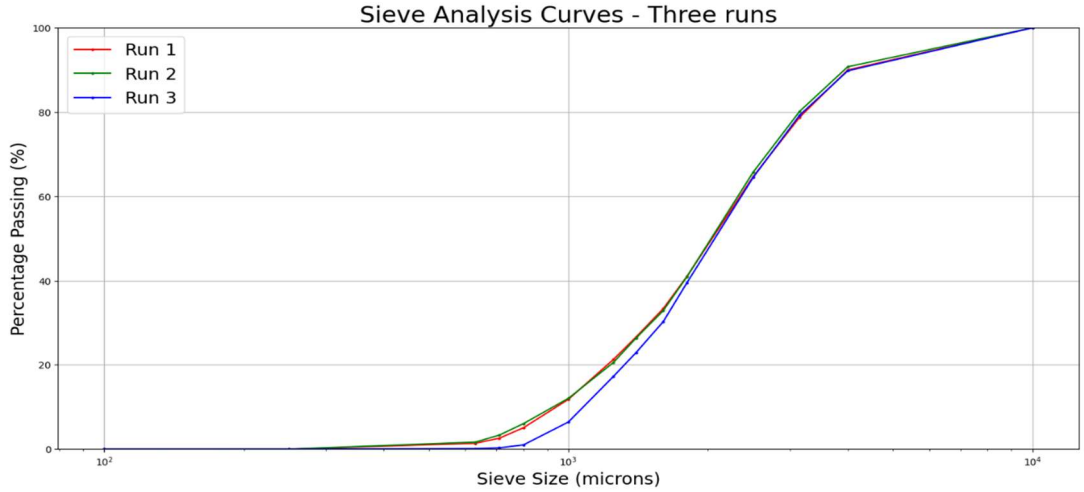

Figure 4.1: Scatter Plot of Sieve analysis curve for three runs.

The curves for first and second runs almost overlapped each other, indicating the precision of the experiment performed while the third one was found slightly deviating. This might have happened, because the sieves were found clogged with small particles of the samples after the first and second runs of test.

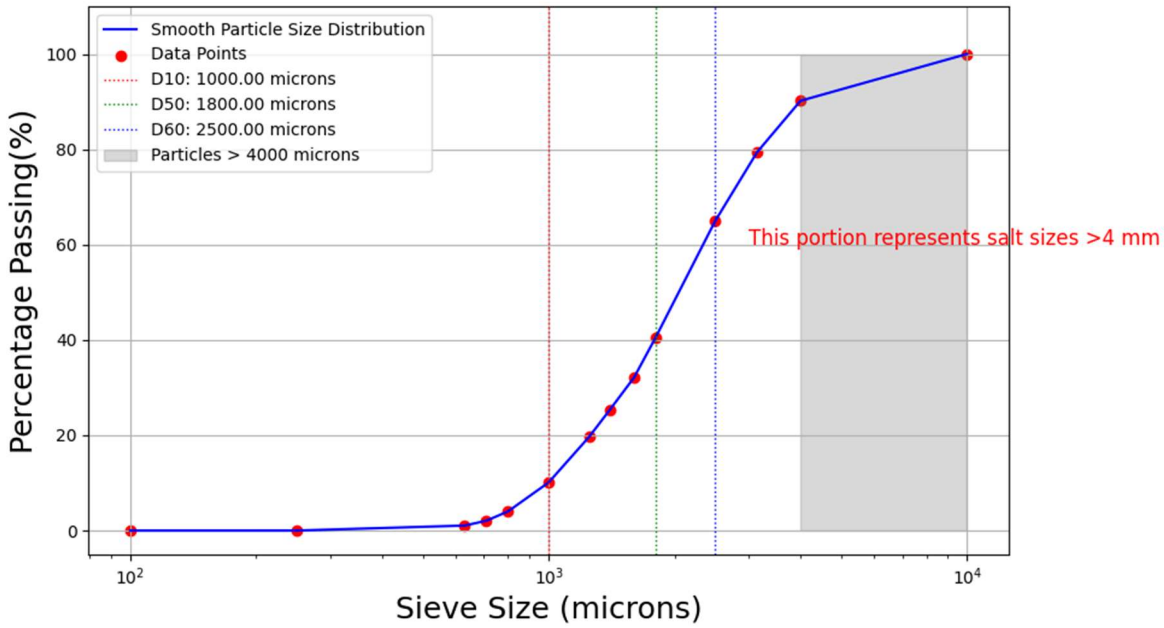

Figure 4.2: Combined Sieve Analysis for three runs.

If we look at the combined curve for the three runs, it was observed that the median salt size was 1800 µm. And the D_{10} and D_{60} were observed to be 1000 µm and 2500 µm. The coefficient of uniformity (C_u) is a measure used in particle size analysis to quantify the uniformity or gradation of a particle size distribution. It is calculated as the ratio of the particle size corresponding to 60% passing to the particle size corresponding to 10% passing (i.e., D_{60} / D_{10}).

$C_u = \frac{D_{60}}{D_{10}}$, which was found to be 2.5. It indicates that the largest salt grain is up to 2.5 times larger than the smallest salt grain size.

Observed combined sieve analysis curves were compared with the other established curves. And it was observed that the salt sizes were somewhere in the range: fine to coarse sand.

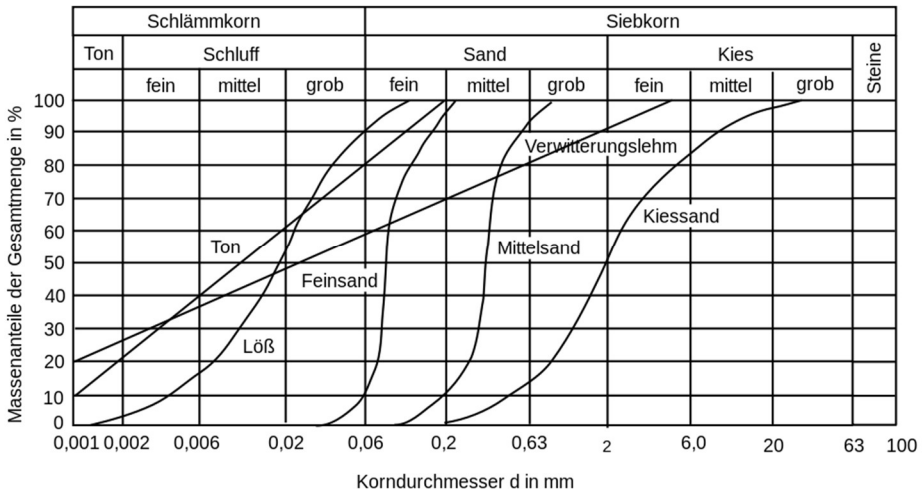

Figure 4.3: Different sieve curves for different sediment particles including clay, salt and sand used to compare the grain size of salt sample (Analysensiebe, Blau-Metall, 2023)

4.2 Experiment on solubility

The saturation point was observed after adding 150 grams of salt to a solution of 500 ml of DW. A little amount of undissolved salt was seen at the bottom of the beaker. To further confirm it, additional 50 grams of salt was added. Further dissolution was not possible. This is observed in figure 3.2(a). Hence, it was deduced that the solubility of salt was in the range of 300 grams to 350 grams per one litre of DW. The room temperature was noted to be 21.5 ℃. Simultaneously at each point of salt addition, parameters like density, temperature, EC and cumulative salt addition were observed.

Rank	Salinity (percentage)	Name	Type	Region or countries
1	44%	Don Juan Pond	Salt lake	Antarctica
2	40%	Lake Retba	Salt lake	Senegal
3	35%	Lake Vanda	Salt lake	Antarctica
4	35%	Garabogazköl	Lagoon	Turkmenistan
5	34.8%	Lake Assal	Salt lake	Djibouti
6	33.7%	Dead Sea	Salt lake	Israel, Jordan, Palestine
7	18%	Little Manitou Lake	Salt lake	Canada
8	8.5–28%	Lake Urmia	Salt lake	Iran
9	5–28%	Laguna Cejar	Salt lake	Chile
10	5–27%	Great Salt Lake	Salt lake	United States
11	5–9.9%	Mono Lake	Salt lake	United States

Figure 4.4: Comparison of Salinity values of different water bodies (Al Bawab et al., 2018).

Table 4.2: Gradual addition of salt sample to raw water (500mL) at 21.5 degrees at constant stirring of 600 rpm with magnetic stirrer.

Initial water taken = 500 ml							
Density(g/L)	Left over crystals?	T(°C)	EC(mS/cm)	Salt(g)	Time till salt is fully dissolved	Cumulative salt(g)	Remarks
0.9464	no	21.5	1	0	0	0	
0.9946	no	21.3	70.7	25	165	25	
1.045	no	20.7	122.4	25	236	50	
1.0942	no	21	162.3	25	521	75	
1.1418	no	21.1	193.3	25	888	100	
1.1914	no	21.4	216	25	984	125	
1.2396	very small	22.4	231	25	1219	150	**Saturation Point**
1.2882	Yes, clearly insoluble	22.6	239	25	1320	175	

Solubility of salt sample = 300g/L- 350 g/L

Upon plotting density vs salt addition, it was found that the density of the salt solution increased linearly with the salt addition. There were fluctuations in the pH values as well. However, due to the poor calibration of pH rods, the reliability for the plot: pH vs salt addition can't be confirmed. The plot of temperature vs salt addition also showed the increment in temperature of the solution. The plot of EC displayed a curve, which flattened at the attainment of the saturation state of the salt solution.

If we compare the salinity values of the saltiest water bodies, Don Juan Pond of the Antarctica is at the first rank. The salinity percentage for the Dead Sea according to figure 4.4 is 33.7 %. The value of solubility calculated from the lab 300 g/L to 350 g/L, meaning the solubility of the salt sample and salinity of the water found in the DS region are comparable.

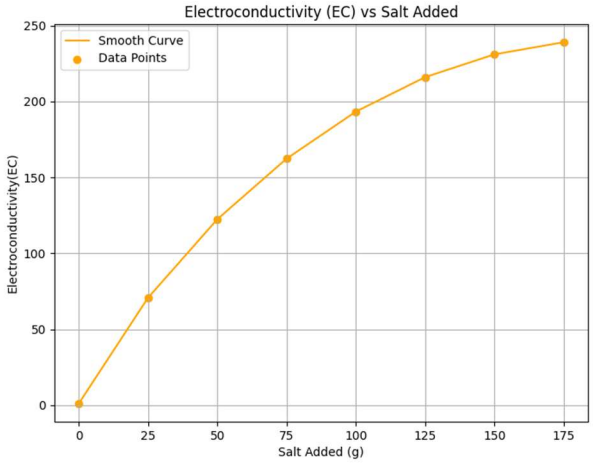

(a)

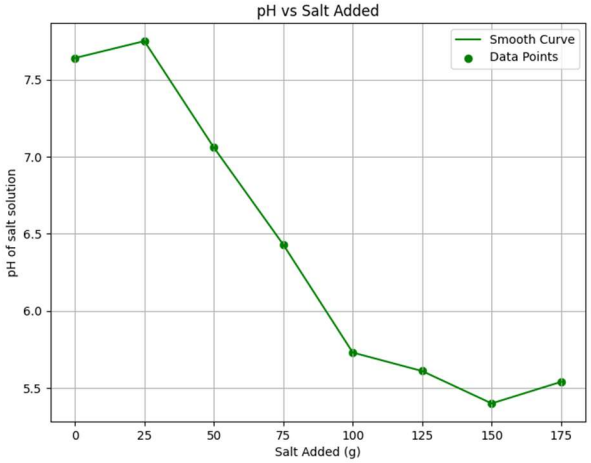

(b)

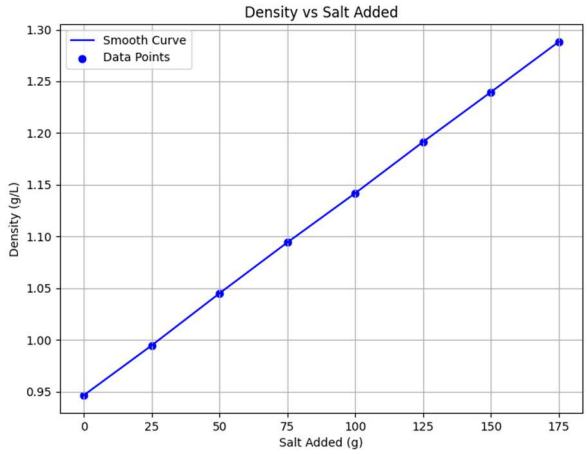

(c)

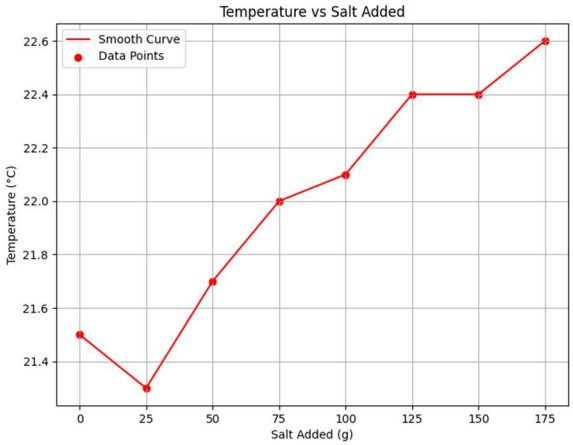

(d)

Figure 4.5: (a) Plot of EC vs salt addition (b) pH vs salt addition (c) Density of salt solution vs. salt added (d) Temperature vs. Salt added

4.3 Calculation of bulk density:

Since density is an important parameter, three samples of random amount of salt sample were taken randomly. The masses of each of the samples were taken alongside with the volume measured with volumetric flask. Finally, the bulk density of each of the sample were calculated as the ratio of mass and volume.

$$Bulk\ Density = \frac{Mass}{Volume}$$

Table 4.3: Calculation of Bulk density for 3 random samples

	weight of vessel(g)	**Volume(ml)**	**weight of vessel including salt(g)**	**Density(kg/m^3)**
sample 1	103.05	200	356.85	1269
sample 2	104.05	150	297.85	1292
sample 3	77.85	500	670.4	1185.1
			Bulk density	**1248.7**

4.4 Settling velocities in brine condition

Since the actual brine conditions as of that present in the DS area couldn't be replicated in the lab, literature was looked up to find the brine water conditions to find the settling velocities for different salt grain sizes. Using the settling velocity formula based on Stoke's law, different settling velocities corresponding to the grain sizes were calculated. It was observed that the salt grains settled rapidly in DW up to velocity of 0.5 m/s while in BW condition, they were found to settle very slowly at a speed of 0.003 m/s to 0.006 m/s.

$$\boldsymbol{V_s = \frac{r^2 g(\rho_s - \rho_{DS})}{18\mu}}$$

Where,

$\boldsymbol{V_s}$ is the settling velocity of the particle (m/s).

$\boldsymbol{\rho_s}$ is the density of the halite (kg/m³).

$\boldsymbol{\rho_{DS}}$ is the density of the brine solution (kg/m³).

$\boldsymbol{g}$ is the acceleration due to gravity (m/s²).

$\boldsymbol{r}$ is the radius of the particle (m).

$\boldsymbol{\mu}$ is the dynamic viscosity of the fluid (kg/(m·s)).

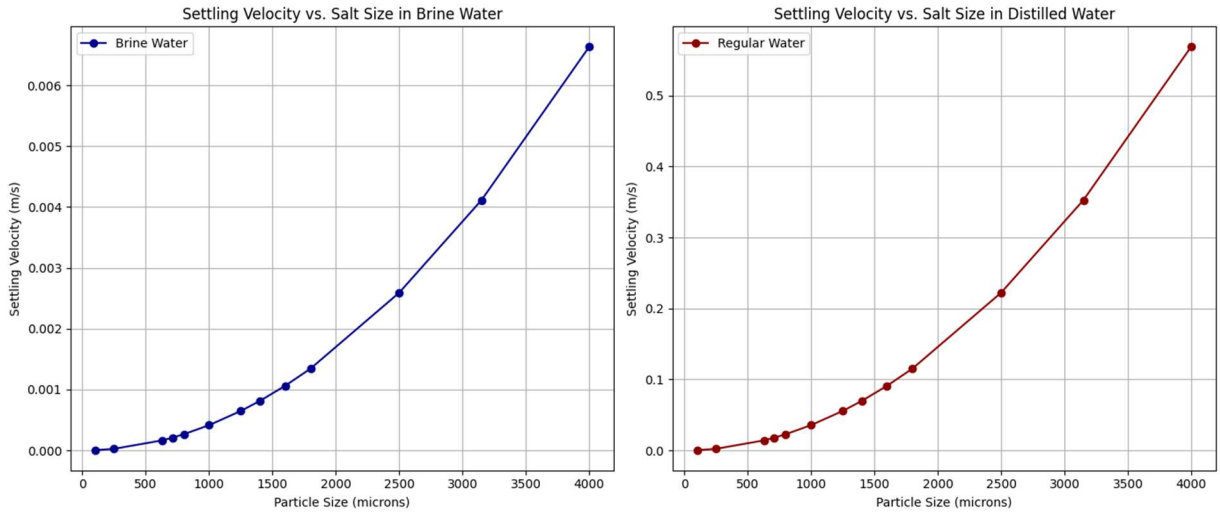

Figure 4.6: Settling velocities of salt particles under BW condition and under DW, respectively.

4.5 Particle Count Analysis

After the end of the solubility test, it was seen that the salt solution was turbid, meaning for the possible presence of undissolved particles. For this, particle counter was employed to find the distribution of particles in the salt solution. For this, 10 ml of the salt solution was fed into particle counter with a cycle of 105 seconds. Then the results were obtained in the computer connected with the particle counter. Following were the obtained results.

Table 4.4: Data for sieve analysis of 3 test runs

Particle size(µm)	Number	Cumulative number	Cumulative Percentage
1	251912	251912	17.76%
2	408748	660660	46.57%
4	492947	1153608	81.31%
8	170444	1324052	93.32%
10	71248	1395299	98.35%
14	18448	1413747	99.65%
20	3175	1416922	99.87%
25	743	1417666	99.92%
30	383	1418049	99.95%
35	200	1418249	99.96%
40	99	1418348	99.97%

45	52	1418400	99.97%
50	23	1418423	99.98%
55	14	1418437	99.98%
60	9	1418446	99.98%
65	6	1418452	99.98%
70	6	1418458	99.98%
80	3	1418461	99.98%
90	2	1418463	99.98%
100	1	1418464	99.98%
110	1	1418465	99.98%
120	1	1418466	99.98%
130	3	1418469	99.98%
140	302	1418771	100.00%

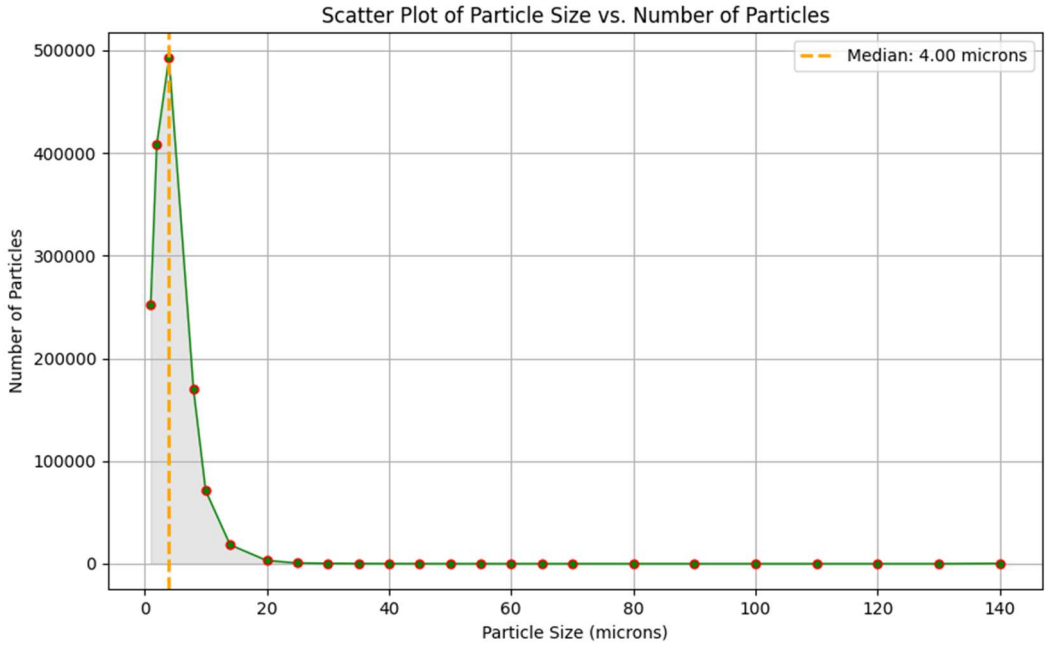

Figure 4.7: Scatter Plot of particle size vs. Number of particles.

It was observed that the median particle size was 4 µm. If we follow different classification schemes as shown in figure 4.8, this size corresponds to the sizes in the range silt to clay.

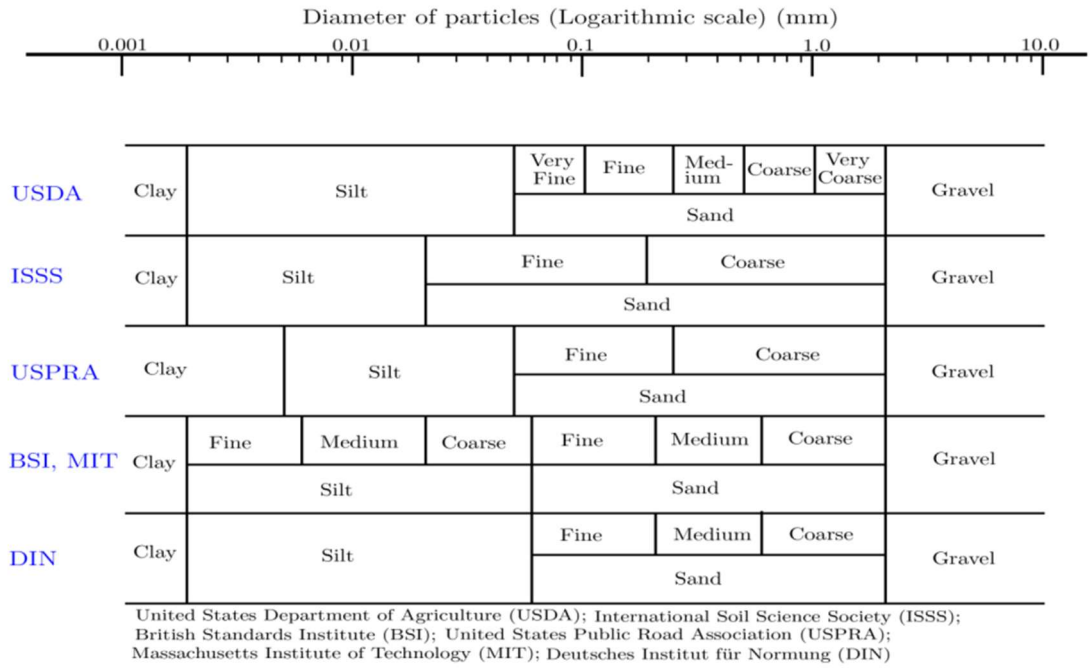

Figure 4.8: Classification schemes to define ranges of grain diameters for clay, silt, sand, and gravel according to DIN, USDA, ISSS,USPRA, BSI and MIT.

4.6 ICP-MS

From ICP-MS, elemental composition of the salt sample was found. To no surprise, the salt had 98.90 % of sodium element. Remaining of the elements were Potassium, Calcium, Iron, Magnesium, and other trace elements. The anions like chloride, sulphate, etc. were not detected in the process. Following observations were found:

Table 4.5: Results obtained from ICP-MS

Element	**Symbol**	**Fraction of element**	
Aluminium	Al	0.08	mg/g
Arsen	As	4.88	µg/g
Bor	B	0.00	µg/g
Barium	Ba	0.00	mg/g
Calcium	Ca	1.43	mg/g
Cadmium	Cd	0.00	µg/g
Cobalt	Co	0.00	µg/g
Chrom	Cr	0.00	µg/g

Kupfer	Cu	12.22	µg/g
Eisen	Fe	0.42	mg/g
Kalium	K	1.53	mg/g
Lithium	Li	4.35	µg/g
Magnesium	Mg	1.03	mg/g
Mangan	Mn	0.02	mg/g
Natrium	Na	418.91	mg/g
Nickel	Ni	4.31	µg/g
Phosphor	P	0.00	mg/g
Blei	Pb	17.06	µg/g
Silicium	Si	0.05	mg/g
Strontium	Sr	9.40	µg/g
Zink	Zn	0.05	mg/g

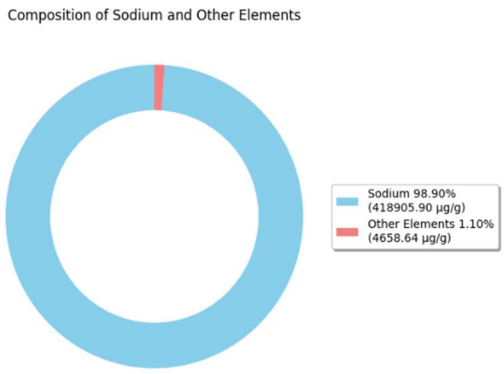

Figure 4.9: Elemental composition of Halite, mostly dominated by Sodium.

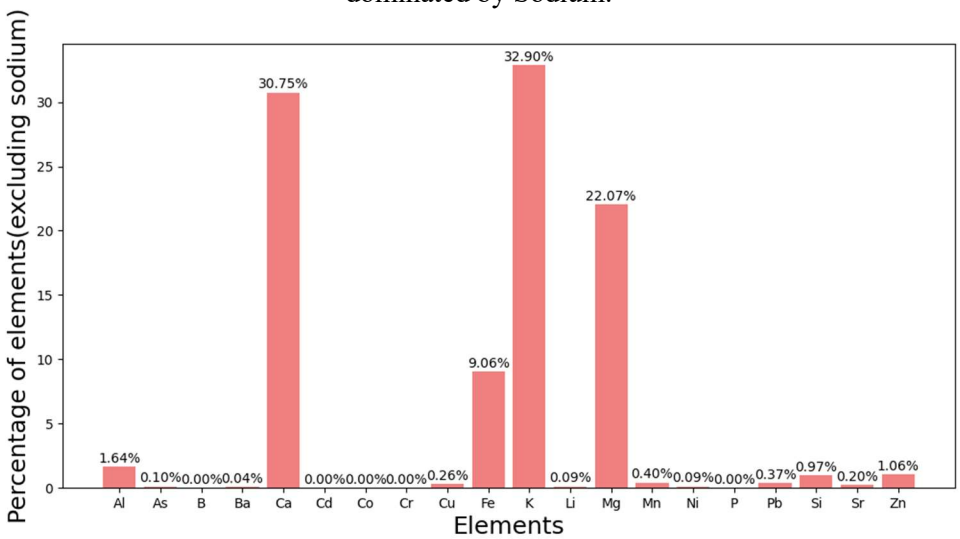

Figure 4.10: Elemental Composition of Halite excluding Sodium.

5. Conclusions

From the study carried out, it was found that the salt grains were in the sizes ranging from 100 microns to 4000 microns with a median size of 1800 microns. The calculated bulk density of salt was approximately 1250 kg/m^3. The elemental composition was sodium primarily consisting of at 98.90% and trace elements such as Fe, Mg, and Al at 1.1%. However, the presence of particulate substances (in the size ranges of silt and clay), that do not dissolve in solution, as indicated by turbidity in diluted salt solutions, poses challenges in utilizing accumulated Halite. This, coupled with the detection of elements like Fe and Al, implies a potential increase in production costs due to the need for additional purification processes. The value of solubility of salt sample and salinity of the water in the DS region was found comparable.

The feasibility of the transportation of salt as granular material through Nahal Arava river to the Northern was difficult to study out because it was extremely hard to find the information related to Nahal Arava river, and the real scenario present in the DS region was difficult to replicate in the laboratory.

6. Outlook/Recommendations

It was difficult to find if it were possible to transport the accumulated halite through Nahal Arava to the Northen basin as a granular material because of the limited resources and information. The information mostly found were from the Geological Survey of Israel (GSI) and most of them were published in Hebrew language.

The real brine solution from the river could be taken and studied out to see and observe more real scenarios. Knowledge of proper flow conditions of the Nahal Arava would help calculate more scientifically the transportation feasibility of salt sample as a granular material.

However, the results of the conducted physical and chemical tests could be handy in continuing the study with more information. The findings of the study could also be used to cross validate the obtained results.

7. Bibliography

Abelson, M., Gabay, R., Shalev, E., & Yechieli, Y. (2009). *Sinkholes hazard around the evaporation ponds* . Geological Survey of Israel.

Al Bawab, A., Bozeya, A., Abu-Mallouh, S., Irmaileh, B. A., Daqour, I., & Abu-Zurayk, R. A. (2018). The Dead Sea Mud and Salt: A Review of Its Characterization, Contaminants, and Beneficial Effects. *IOP Conference Series: Materials Science and Engineering*, p. 305. https://doi.org/10.1088/1757-899X/305/1/012003

Eyal, H., Dente, E., Haviv, Y., Dunne, T., & Lensky, N. G. (2019). Fluvial incision and coarse gravel redistribution across the modern Dead Sea shelf as a result of base-level fall. *Earth Surface Processes and Landforms, 44*, 2170-2185. https://doi.org/10.1002/esp.4640

Gavrieli, I., Calvo, R., & Lensky, N. (2009). *Alternative dumping sites in the Dead Sea for harvested salt from pond 5.* Geological Survey of Israel.

Lensky, N., Dvorkin, Y., Lyakhovsky, V., Gertman, I., & Gavrieli, I. (2005). Water, Salt, and Energy Balances of the Dead Sea. *Water Resources Research, 41*(W12418). https://doi.org/10.1029/2005WR004084

Reznik, J. R., & Gavrieli, I. (2023). Massive-Scale Dissolution, Conveyance, and Disposal of Dead Sea. *Environmental Sciene and Technology, 57*, 8385-8395. https://doi.org/10.1021/acs.est.3c01197

Sztankeler, V., Meir, I. A., & Schwartz, M. (2012). Physical Development in an Ecologically Sensitive Area: The Planning of the Dead Sea Region. In *Geography Research Forum* (pp. 119-145).